



Desulphurization of Simulated Oil Using SAPO-11 with CNT's as Adsorbent: A Kinetic Study

Gaith K. Jabaar ^{a,*}, Haider A. Al-Jendeel ^a, Yasir Ali Alsheikh ^b

^a Chemical Engineering Department, College of Engineering, University of Baghdad, Baghdad, Iraq

^b Department of Chemical & Petrochemical Engineering, University of Nizwa, Initial Campus, Birkat Al Mouz, Nizwa, Sultanate of Oman

Abstract

In this study, sulfur was removed from imitation oil using oxidative desulfurization process. Silicoaluminophosphate (SAPO-11) was prepared using the hydrothermal method with a concentration of carbon nanotubes (CNT) of 0% and 7.5% at 190 °C crystallization temperature. The final molar composition of the as-prepared SAPO-11 was Al_2O_3 : $0.93\text{P}_2\text{O}_5$: 0.414SiO_2 . 4% MO/SAPO-11 was prepared using impregnation methods. The produced SAPO-11 was described using X-ray diffraction (XRD) and Brunauer-Emmet-Teller (N_2 adsorption-desorption isotherms). It was found that the addition of CNT increased the crystallinity of SAPO-11. The results showed that the surface area of SAPO-11 containing 7.5% CNT was $179.54 \text{ m}^2/\text{g}$, and the pore volume was $0.317 \text{ cm}^3/\text{g}$. However, the surface area of SAPO-11 containing 0% CNT was $125.311 \text{ m}^2/\text{g}$, and pore volume was $0.275 \text{ cm}^3/\text{g}$, while nanoparticles with an average particle diameter of 24.8 nm were obtained. Then, the prepared SAPO-11 was used in the oxidative desulfurization process. The oxidative desulfurization was studied using several factors affecting desulfurization efficiency, such as time (40, 60, 80, 100, and 120) min, amount of MO/SAPO-11 (0.3, 0.4, 0.5, 0.6, and 0.7) g/100 ml of simulated oil (100 ppm of dibenzothiophene), the amount of hydrogen peroxide (4ml) oxidizer/100 ml of simulated oil, and the temperature ranges from (40, 50, 60, 70, and 80 °C). The results showed that an increase in MO/SAPO-11 led to an increase in desulfurization. The best removal percentage for sulfur content was 92.79%, obtained at 70 °C and 0.6 g of MO/SAPO-11 containing 7.5% CNT, and the removal was 82.34% at 0% CNT and the same other conditions. While the equilibrium was achieved after 100 min. The results revealed that Freundlich's model described the adsorption of sulfur compounds better than Langmuir's, where the R^2 of the Freundlich model was 0.9979 and the R^2 of the Langmuir model was 0.9554.

Keywords: carbon nanotubes; Desulfurization; isotherms; surface area; pore size distribution; SAPO-11.

Received on 11/01/2023, Received in Revised Form on 05/02/2023, Accepted on 07/02/2023, Published on 30/09/2023

<https://doi.org/10.31699/IJCPE.2023.3.7>

1- Introduction

In recent years, concerns pertaining to the environment have garnered an increasing amount of attention. SO_x is one of the contaminants that has contributed to harmful impacts on the environment [1]. The majority of sulfur oxides are produced from the burning of sulfur-containing substances that are found in gasoline and diesel fuel [2]. As a consequence of this, reducing the amount of sulfur found in transportation and improving the industry's fuel efficiency should be a top priority for the oil business. Benzothiophene (BT), dibenzothiophene (DBT), and 4,6-dimethyl dibenzothiophene are examples of aromatic sulfur-containing compounds [3]. It is common knowledge that these chemicals can cause cancer [4]. In addition, the byproducts of these reactions also contribute significantly to increase the overall sulfur level of fuel. Nevertheless, the industrial norms that are currently in place. The removal of refractory chemicals, such as 4-methyl dibenzothiophene (4-MDBT) and 4,6-dimethyl dibenzothiophene (DMDBT), was less successful when using the hydrodesulfurization (HDS) approach (R) [5]. The sulfur component is often present in negligible

amounts in naphtha [8]. The conditions of this treatment method include high temperatures and high hydrogen pressure [6]. Then, as a method that works in tandem with HDS, oxidative desulfurization, also known as ODS, has been the subject of substantial research [7]. This sulfur causes a number of issues, including equipment wear, catalyst poisoning, processing disruption, oxidation of sulfur compounds to sulfur oxides during fuel combustion, and disruption of sulfur compounds. Sulfur can be found in concentrations between a few hundred and thousands of parts per million. Environmental rules have been proposed to drastically lower the sulfur content of distilled fuels (10 ppm)[8]. The goal is to reduce dangerous exhaust emissions from gasoline-powered vehicles and enhance air quality. Other methods have been developed to lower the sulfur concentration in liquids, including hydro-desulfurization (HDS), oxidative desulfurization (ODS), adsorption desulfurization (ADS), bio-desulfurization (BDS), and extractive desulfurization (EDS) [9]. To produce fuels with extremely low levels of sulfur, the HDS process requires harsh processing conditions. ODS has received increasing attention as a



new method for deep desulfurization of light oil because achieving lower sulfur content in fuels with current hydrogen desulfurization (HDS) technology requires the use of a higher reaction temperature, higher reaction pressure, and a larger reactor volume [10]. There are also some problems inherent in HDS in the conversion of heterocyclic sulfur compounds such as methylated derivatives of DBT, 4-methyldibenzothiophene and 4,6-dimethylbenzothiophene (4,6DMDBT) [11]. ODS operates at atmospheric pressure and temperatures below 100 °C, resulting in moderate reaction conditions, no hydrogen requirement, no pressure reactor, and unique operating technology. ODS can remove nitrogen at the same time, and it has high selectivity, so that sulfur compounds (BT, DBT, etc.) that are difficult to remove can be easily removed by oxidation [3]. Sulfur-containing compounds are oxidized using selective oxidizing compounds that can be preferentially extracted from light oil due to their increased relative polarity, and these oxidizers include peroxyorganic acids, hydroperoxides, nitrogen oxides, peroxyates, and ozone [12]. These compounds can donate oxygen atoms to sulfur in

mercaptans (thiols), sulfides, disulfides, and thiophene to form sulfoxides or sulfonates. Oxidation is achieved by contacting an oxidant with a light oil under optimal conditions and continuing the reaction until the formation of oxidizing compounds containing sulfonates [13]. The sulfonates formed from the oxidation are not only removed in the aqueous phase, but also form an insoluble precipitate and remain in the light oil. Oxidizing compounds can be extracted from light oil by contacting the light oxidized oil with an immiscible solvent [14]. The aim of this work was to study the effect of carbon nano tubes (CNT's) in Mo/SAPO-11 catalysts and examine its activity in oxidative desulfurization of simulated oil (DBT) with four main variables CNT amount, time, temperature, and amount of adsorbent [15].

2- Experimental

2.1. Materials

Table 1 shows the materials used in the synthesis of MO/ SAPO-11 and in the desulfurization process.

Table 1. Properties of Chemicals Used

| Material | Formula | Purity% | Supplier |
|------------------------|--|---------|------------------------|
| n-Hexane | CH ₃ (CH ₂) ₂ CH ₃ | 99 | CDH, India |
| Carbon nanotubes SWNTs | (NH ₄) ₆ H ₂ W ₁₂ O ₄₀ | 90 | United States |
| Acetic acid | CH ₃ COOH | 98 | CDH, India |
| Aluminum isopropoxide | Al [OCH(CH ₃) ₂] ₃ | 100 | BDH |
| Phosphoric acid | H ₃ PO ₄ | 85 | pomerac, Spain |
| Silica sol | SiO ₂ | 99.9 | Qingdao Jigidas, China |
| Di n-propylamine | C ₆ H ₁₅ N | 99 | BDH |
| Hydrogen peroxide | H ₂ O ₂ | 50 | Pomerac, Spain |
| Acetonitrile | C ₂ H ₃ N | 99 | CDH, India |
| Molybdic Acid | MoO ₃ | 87 | BDH, England. |
| dibenzothiophene | C ₁₂ H ₈ S | 99 | BDH, England. |

2.2. Catalysts Preparation

SAPO-11 was prepared by adding 4.61 g of phosphorous acid as a source of phosphorus to 46.72 g of distilled water [16]. These components were thoroughly blended together for 30 minutes to produce a smooth, uniform mixture. Then, 8.17 g of aluminum isopropoxide was added and stirred for 2 hours. After that 1.47 g of di-n-propylamine was injected into the gelatin mixture as a structure-directing template followed by the addition of 1.385 g of silica sol as a source of Si. It took two hours of stirring to create the reaction mixture. Crystallization was performed in a stainless steel autoclave which is a stainless steel cylinder with a thickness of 3 mm made from st.st.310, a Teflon-lined Teflon insert, and a Teflon insert with a hat design cup configuration with a thickness of 7 mm on the side cylindrical part and 10 on the bottom.

The crystallization was performed for 24 hours at 190 °C. It was then left to mature for an additional four hours at room temperature without stirring. Then, the sample was filtered and washed several times to remove impurities from the sample and then dried for 24 hours at 110°C. Then, the raw powders were calcined at 550 °C for three hours in furnaces before being cooled. The powder form of the molecular sieve was then obtained and saved in desiccators. After calcination, the molar composition of the molecular sieve is Al₂O₃:0.93P₂O₅:0.414SiO₂ [17]. All the procedure above was repeated using 7.5% CNTs. After preparation molybdenum was loaded onto SAPO 11 using the impregnation method by adding Molybdic acid drop by drop to SAPO-11 powder under vacuum (0.9 bar) for 60 minutes with manual shaking, followed by drying the formed solution in a furnace at a temperature of 110 °C for 24 hours. Finally, it was exposed to calcination at

550°C for 3 hour [18]. Then, 0.696 g of MoO₃ was dissolved in the required weight of water for impregnation until the volume of the solution equals a pore volume of 20 g (ie 12.8 ml) at 60 °C to allow the solution to easily permeate into the solid catalytic core. The impregnated materials were then dried at 110 °C for 2 hours before being calcined in an oven at 550°C for 3 hours with dry air [19].

2.3. Characterization of catalysts

The produced samples were examined using a Shimadzu SRD 6000 X-ray diffractometer (XRD) from Japan with a fixed power source of 40Kv, 30mA, and a Cu wavelength radiation of 1.54060 cm⁻¹ in the 2theta range of (5-60) C°. At the Petroleum Research and Development Center by the Ministry of Oil, the surface area and pore volume of all prepared samples were measured using the Brunauer, Emmett, and Teller (BET) technique on a Thermo Analyzer/USA. The ASTM D1993 specification's standards were followed in the execution of these measurements. Fig. 1 shows XRD of the prepared MO/SAPO-11 with different CNT (0% and 7.5%)

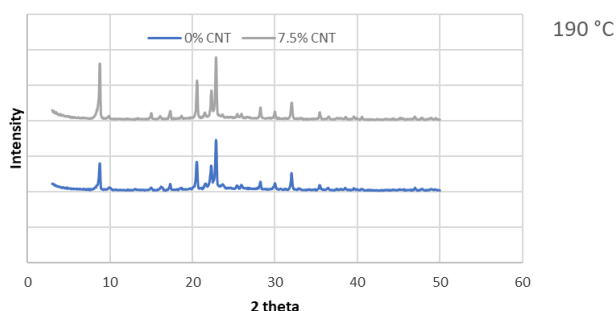


Fig. 1. XRD Diffraction MO/SAPO-11 at 190°C and 550 °C Calcination Temperature

2.4. Oxidation desulfurization of Simulated oil

A sample volume of 100 mL of an n-hexane solution containing a concentration of 100 ppm DBT was placed in a three-neck round flask reactor with a condenser. The reactor was spun at a constant mixing speed of 150 rpm and heated to 40, 50, 60, 70, and 80 °C using a magnetic stirrer heater. After the reaction mixture reached the desired temperature, 4 ml of hydrogen peroxide as an oxidizing agent and 1 ml of acetic acid were added each time (40, 60, 80, 100, and 120 min), and different amounts of MO/SAPO-11 (0.3, 0.4, 0.5, 0.6, 0.7 g) were added. Then, the solution was allowed to settle in a 100 ml separation funnel before 10 ml of the organic solvent acetonitrile was added to separate the phases, giving distinct and recognizable results. Then the material was extracted from the organic phase [20].

3- Results and Discussion

Pretreatment of the solution of the prepared SAPO-11 by adding carbon nanotubes (MWNTs) then

crystallization the solution at 190 °C can make the zeolite in the form of carbon nanotubes with a surface area of 179.54 m²/g, 0.317 cm³/g pore volume and average particle diameter of 24.8 nm which are much smaller particles and large surface area compared to the catalyst synthesized by standard methods. SAPO-11 nanoscale prepared using the improved method not only resulted in a wide surface area but also a large distribution of nanoparticles and crystallinity. While SAPO-11 was prepared without carbon nanotubes showed a surface area of 125.311 m²/g and a pore volume of 0.275 cm³/g.

3.1. The effect of adding carbon nanotubes to MO/SAPO-11 on desulfurization

As demonstrated in Fig. 2, the utilization of MO/SAPO-11 with 7.5% CNT and without carbon nanotubes showed a different manner. The inclusion of carbon nanotubes into MO/SAPO-11 increased sulfur compound elimination and, thus, surface area. This increase in surface area increased the number of active sites and enhanced the oxidation processes for sulfur removal [14]. The findings reveal that the desulfurization process is significantly enhanced when SAPO-11 is combined with CNT.

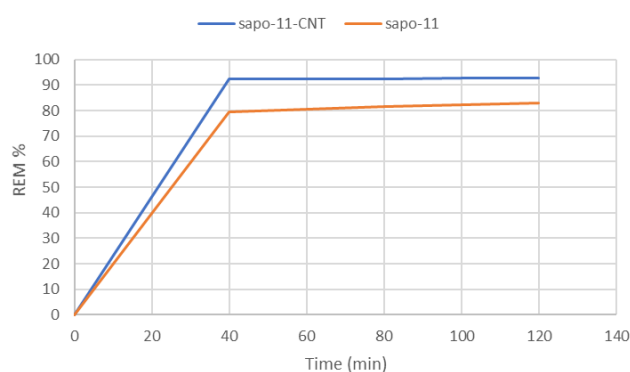


Fig. 2. Effect of CNT in MO/SAPO-11 Quality on Removal of Sulfur Compounds at 0.6 G at 70 °C

SAPO-11 CNT surface area of 179.54 (m²/g), 0.317 (cm³/g) pore volume. SAPO-11 surface area 125.311 m²/g, pore volume 0.275 cm³/g.

3.2. The effect of reaction time

The effect of reaction time (0-120 min) on the removal of sulfur from simulated oil was studied at various temperatures (40, 50, 60, 70, 80) °C, constant amount of H₂O₂, and acetic acid of 4 ml and 1 ml respectively and 7.5% CNT, as shown in Fig. 3. This figure showed that desulfurization was a function of reaction time. By extending the reaction time, the outcomes are enhanced. This may be explained by discussing how oxidizing agents interact with time [21]. Dibenzothiophene reacts with H₂O₂ and acetic acid to generate a sulfonate which like any other reaction requires sufficient time to complete and solidify over time [22]. also the high surface area of MO/SAPO-11 increase the adsorption of sulfur

compounds, so at the beginning the driving force was large enough for adsorption process making a rapid adsorption within the first 40 min, after that the decrease in concentration gradient lead to a decrease in adsorption process. The optimal REM% was obtained 100 min after treatment [23]. Similar behavior was obtained by Beshkoofeh et al. [24]. In this study phosphomolybdic

acid catalyst was used to remove the oxidized sulfur of a typical sulfur compound, which made the residual sulfur content decreasing with increasing oxidation time. The reaction closed to equilibrium after 100 min, and the residual sulfur content was almost unchanged. Table 2 shows the amount of sulfur removal with time for each temperature.

Table 2. Shows the Amount of Sulfur Removal with Time for each Temperature

| 40 °C | | 50 °C | | 60 °C | | 70 °C | | 80 °C | |
|------------|-------|------------|-------|------------|-------|------------|-------|------------|-------|
| Time (min) | REM % | Time (min) | REM % | Time (min) | REM% | Time (min) | REM% | Time (min) | REM% |
| 40 | 84.87 | 40 | 86.78 | 40 | 90.34 | 40 | 92.24 | 40 | 83.45 |
| 60 | 86.38 | 60 | 88.56 | 60 | 91.4 | 60 | 92.33 | 60 | 84.3 |
| 80 | 90.18 | 80 | 90.5 | 80 | 91.48 | 80 | 92.45 | 80 | 85.45 |
| 100 | 91.22 | 100 | 91.37 | 100 | 92.56 | 100 | 92.78 | 100 | 87.3 |
| 120 | 91.25 | 120 | 91.42 | 120 | 92.58 | 120 | 92.80 | 120 | 87.32 |

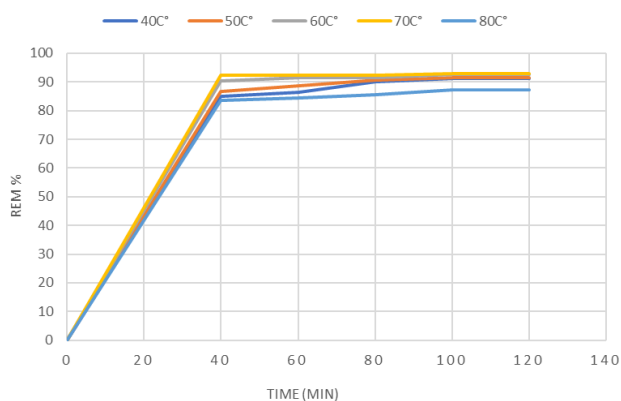


Fig. 3. The Effect of Reaction Time on DBT Removal at Different Temperatures with 7.5% CNT

3.3. The effect of reaction temperature

The effect of the reaction temperature on the desulfurization efficiency was investigated at a fixed reaction time of 100 minutes at 40°C, 60°C, 70°C and 80°C. At these temperatures, the amount of hydrogen peroxide 4% by volume was fixed with different amounts of MO/SAPO-11 (0.3,0.4,0.5,0.6,0.7 gm) of 7.5% CNT as shown in Fig. 4. The obtained results indicated an improvement in the oxidation of sulfur compounds to sulfone oxide and sulfonate with increasing the reaction temperature from 40 °C to 70 °C, and thus an improvement in the desulfurization efficiency was observed. At 40 °C, desulfurization was less than at 60 °C and 70 °C. The increase in the reaction temperature promotes the oxidation of the present thiophene compounds. This may be related to the decomposition of hydrogen peroxide with the increase in the reaction temperature producing hydroxyl radicals that act as a strong oxidizing agent. Therefore, 70 °C was chosen as the optimal reaction temperature considering that a higher temperature did not show an additional beneficial effect on desulfurization [25]. The same behavior was observed by several researchers, such as Lanju et al., [26] who studied the oxidation of thiophene using silica gel in

hydrogen peroxide and formic acid system, and found that desulfurization rates improved as the temperature exceeded 50 °C. Also, Ahmedzaki and Ibrahim [27], found that the best results occurred at 70 °C because increasing the temperature accelerated the reaction rate.

3.4. The effect of the amount of MO/SAPO-11 on Desulfurization Process

An increase in the mounts of MO/SAPO-11 led to an increase in the desulfurization efficiency because oxidation rates increased by increasing the attraction of the organosulfur compounds to the aqueous phase where the oxidation takes place. This behavior was also indicated by [28]. The efficiency of MO/SAPO-11 on the removal of sulfur and desulfurization efficiency was shown in Fig. 5. When the amount of SAPO-11 increased from 0.3 to 0.6, the percent of removal increased and this was due to the high surface area of MO/SAPO-11 which means increasing the dosage led to more area for adsorption of sulfur compounds. On the other hand, increasing the amounts of MO/SAPO-11 from 0.6 g to 0.7 g led to an increase in the removal rate.

4- Study of Adsorption Isotherms

This study was conducted using the MO/SAPO-11 catalyst, initial DBT concentration in the 100 mL of n-hexane solution used for the batch procedure was 100 ppm. The solution was kept agitated so that sulfur penetrates uniformly throughout a reaction media. The concentration of sulfur in solution was measured as a function of time at certain temperatures. Using Eq. 1 [29], the quantity of sulfur adsorbed on the catalyst was determined.

$$q_e = (C_o - C_e) * v / m \quad (1)$$

q_e : the amount of sulfur adsorbed at equilibrium on MO/SAPO-11 (mg. g⁻¹), C_o : initial concentration of

sulfur in solution (mg. L^{-1}), C_e : concentration of sulfur in solution at equilibrium (mg L^{-1}), m : mass of catalyst (g),

V : volume of the solution (L).

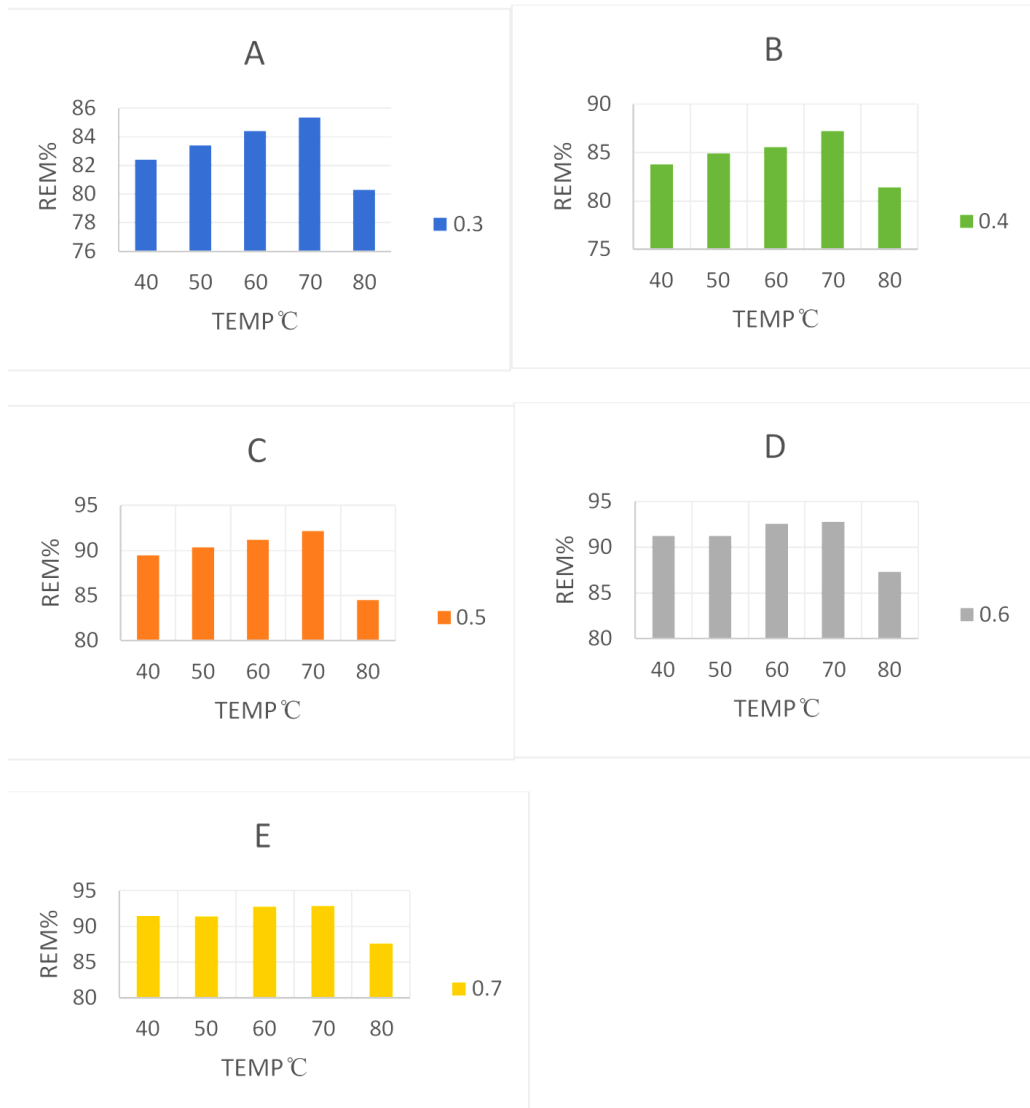


Fig. 4. Effect of Reaction Temperature on the Removal of DBT in Different Amounts of MO/SAPO-11 (A 0.3 g, B 0.4 g, C 0.5 g, D 0.6 g, E 0.7 g) With 7.5% CNT at 70°C

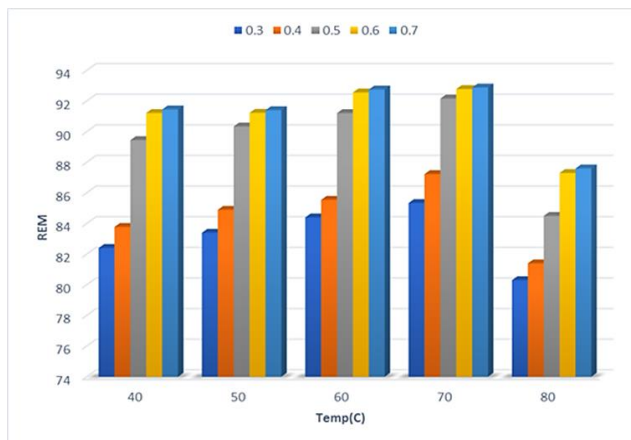


Fig. 5. Effect of Reaction Temperature on the Removal of DBT in Different Amounts of MO/SAPO-11

4.1. Langmuir isotherm model

The Langmuir model permits the determination of whether a monolayer is adsorbed otherwise no contact between the adsorbed molecules. The Langmuir equation is true for just one monolayer adsorbed with a well-defined number of energetically identical and uniform adsorption sites, as shown in Eq. 2 [30]

$$C_e/q_e = 1/(q_o \cdot b) + 1/q_o \quad C_e \quad (2)$$

Where: C_e = the equilibrium concentration of adsorbate (mg/L^{-1}). q_e = the amount of metal adsorbed per gram of the adsorbent at equilibrium (mg/g). q_o = the maximum monolayer coverage capacity (mg/g) b = the slope and intercept of the plot C_e/q_e .

By fitting the experimental findings for the three examined temperatures using the Langmuir equation, the

isotherms shown in Fig. 6 are obtained. The equilibrium parameter RL given by Eq. 3, also known as the separation factor or equilibrium parameter, is a dimensionless constant that can be used to express the fundamental characteristics of the Langmuir isotherm.

$$RL = \frac{1}{1+(1+KL/C_0)} \quad (3)$$

KL = the constant related to the energy of adsorption (Langmuir Constant). RL value indicates whether the adsorption is irreversible if RL= 0, linear if RL=1, favorable if RL > 1), or unfavorable if RL < 1 [29]. RL of 0.2129 was above than 0 but less than 1 indicating that Langmuir isotherm is favorable.

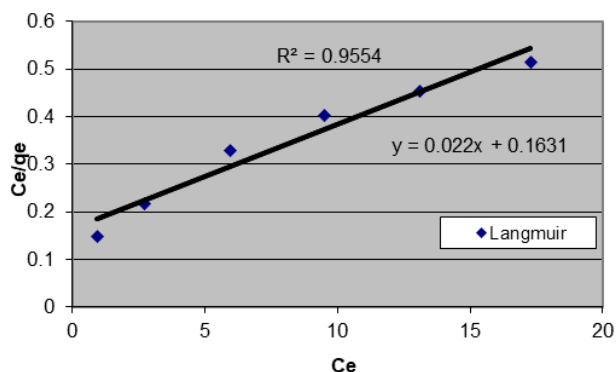


Fig. 6. Langmuir Isotherm Models for Adsorptive Desulfurization of DBT on SAPO-11

4.2. Freundlich isotherm model

The Freundlich model, which represents heterogeneity at the adsorbent surface, was used to calculate adsorption capacity using Eq. 4 [30]:

$$\ln q_e = \ln K_f + \frac{1}{n} \ln C_e \quad (4)$$

Where K_f = denotes the Freundlich isotherm constant (mg/g). n = adsorption intensity. C_e = adsorbate equilibrium concentration (mg/L) at equilibrium. q_e = the amount of metal adsorbed per gram of the adsorbent at equilibrium (mg/g).

According to the following relationship, the linear version of the Freundlich equation can be used in a logarithmic form [31].

Fig. 7 indicates that the adsorption isotherms match the Freundlich model, that the experimental findings can be connected to the Freundlich equation, and that the correlation coefficients are near unity [32]. The Freundlich constants K and n were determined based on the isotherms, and their values are shown in Table 3. Given that the value of n for MO/SAPO-11 was between 1 and 10, this model is suitable for these types of catalysts.

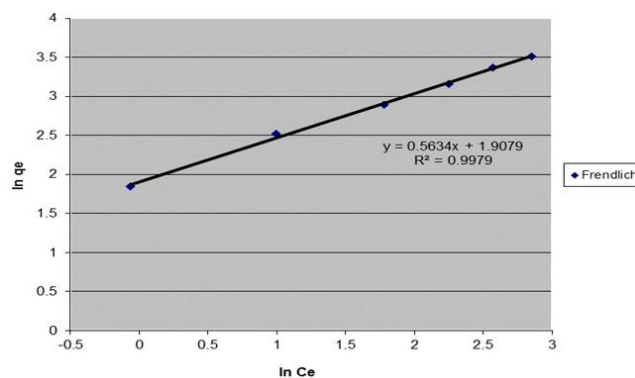


Fig. 7. Freundlich Isotherm Models for Adsorptive Desulfurization of DBT On SAPO-11

Table 3. Adsorption Isotherm Parameters and Correlation Coefficient of SAPO-11

| Isotherm | parameter | Value |
|------------|---|-------------------------|
| | | Simulated fuel with DBT |
| Langmuir | K_L | 0.13488657 |
| | q_0 | 45.4545455 |
| | R^2 | 0.9554 |
| Freundlich | K_F , [(mg/g) (l/mg) ^{1/n}] | 6.738922 |
| | n | 1.774938 |
| | R^2 | 0.9979 |

5- Conclusions

The physical characterization showed that CNT's have been successfully used to develop SAPO-11 crystals compared to the standard approach. The XRD phase pattern and FTIR chemical composition indicated obtaining Mo/SAPO-11 catalyst which indicates efficient use of CNT's for crystal growth. Compared to the typical procedure, Mo/SAPO-11 with a small size of 24.8 nm was generated using CNT's as a crystal growth medium. The efficacy of desulfurization by oxidation was improved by increasing the reaction temperature to 60 °C and duration. Hydrogen peroxide of 4 ml and 1 ml of acetic acid, and 100 minutes are the preferred working conditions. Formation of free radicals was necessary for the oxidation process in the presence of the catalyst, where the reaction takes place on the catalyst's surface. When MO/SAPO-11 was used without carbon nanotubes, the best removal rate was 82.78%, while it was 92.79% when MO/SAPO-11 was used with 7.5% carbon nanotubes. This indicated that using carbon nanotubes with SAPO-11 increased the removal rate by 10%.

References

- [1] N. Yadav, V. K. Garg, A. K. Chhillar, and J. S. Rana, 2021, "Detection and remediation of pollutants to maintain ecosustainability employing nanotechnology: A review," *Chemosphere*, vol. 280, 130792, <https://doi.org/10.1016/j.chemosphere.2021.130792>

- [2] T. A. Saleh, 2020, "Characterization, determination and elimination technologies for sulfur from petroleum: Toward cleaner fuel and a safe environment," *Trends in Environmental Analytical Chemistry*, vol. 25, e00080, <https://doi.org/10.1016/j.teac.2020.e00080>
- [3] S. Palanisamy, D. Palanisamy, M. Gul, K. Kandasamy, and B. S. Gevert, 2021, "Hydro-treating and Hydro-isomerisation of Sunflower Oil using Pt/SAPO-11: Influence of Templates in Ultrasonic Assisted with Hydrothermal Synthesis," *Bulletin of Chemical Reaction Engineering & Catalysis*, vol. 16, no. 1, pp. 120–135, <https://doi.org/10.9767/bcrec.16.1.9889.120-135>
- [4] N. Venkatathri, R. Srivastava, 2004, "Synthesis, characterization and catalytic properties of sapo-11, -31 and -41 molecular sieves, Studies in Surface Science and Catalysis, Volume 154, Part A, Pages 978-984," [https://doi.org/10.1016/S0167-2991\(04\)80913-3](https://doi.org/10.1016/S0167-2991(04)80913-3)
- [5] X. Chen, A. Vicente, Z. Qin, V. Ruaux, J. P. Gilson, and V. Valtchev, 2016, "The preparation of hierarchical SAPO-34 crystals via post-synthesis fluoride etching," *Chemical Communications*, vol. 52, no. 17, pp. 3512–3515, <https://doi.org/10.1039/C5CC09498D>
- [6] A.S. Yaro, M.H. Al-Hassani, H.A.K. Rasheed, 2015, "Treatment copper biosorption using local Iraqi natural agents", *Desalination Water Treat.* 54, 533-539, <https://doi.org/10.1080/19443994.2014.884941>
- [7] A. Ishihara, D. Wang, F. Dumeignil, H. Amano, E. W. Qian, and T. Kabe, 2005, "Oxidative desulfurization and denitrogenation of a light gas oil using an oxidation/adsorption continuous flow process," *Appl Catal A Gen*, vol. 279, no. 1–2, pp. 279–287, <https://doi.org/10.1016/j.apcata.2004.10.037>
- [8] S. Askari, A. Bashardoust Siahmard, R. Halladj, and S. Miar Alipour, 2016, "Different techniques and their effective parameters in nano SAPO-34 synthesis: A review," *Powder Technology*, vol. 301. Elsevier B.V., pp. 268–287. <https://doi.org/10.1016/j.powtec.2016.06.018>
- [9] A. W. Bhutto, R. Abro, S. Gao, T. Abbas, X. Chen, and G. Yu, 2016, "Oxidative desulfurization of fuel oils using ionic liquids: A review," *J Taiwan Inst Chem Eng*, vol. 62, pp. 84–97, <https://doi.org/10.1016/j.jtice.2016.01.014>
- [10] P. de Filippis and M. Scarsella, 2003, "Oxidative Desulfurization: Oxidation Reactivity of Sulfur Compounds in Different Organic Matrixes," *Energy and Fuels*, vol. 17, no. 6, pp. 1452–1455, <https://doi.org/10.1021/ef0202539>
- [11] H. Mohamed, S. Rahman, S. Ahmad Imtiaz, and Y. Zhang, 2020, "Oxidative-Extractive Desulfurization of Model Fuels Using a Pyridinium Ionic Liquid. ", *ACS Omega*, 5, 14, 8023–8031. <https://doi.org/10.1021/acsomega.0c00096>
- [12] I. V Babich, J. A Mouljn, 2003, "Science and technology of novel processes for deep desulfurization of oil refinery streams: a review, *Fuel*, 82(6), 607-631, [https://doi.org/10.1016/S0016-2361\(02\)00324-1](https://doi.org/10.1016/S0016-2361(02)00324-1)
- [13] B. Rodríguez-Cabo, H. Rodríguez, E. Rodil, A. Arce, and A. Soto, 2014, "Extractive and oxidative-extractive desulfurization of fuels with ionic liquids," *Fuel*, vol. 117, no. PART A, pp. 882–889, <https://doi.org/10.1016/j.fuel.2013.10.012>
- [14] Javadli, R., de Klerk, A. 2012, "Desulfurization of heavy oil". *Appl Petrochem Res* 1, 3–19. <https://doi.org/10.1007/s13203-012-0006-6>
- [15] Mousa, H. J., and Hussein, H. Q. Adsorptive Desulfurization of Iraqi Heavy Naphtha Using Different Metals over Nano Y Zeolite on Carbon Nanotube. *Iraqi Journal of Chemical and Petroleum Engineering*, 21(1), 23–31, 2020, <https://doi.org/10.31699/IJCPE.2020.1.4>
- [16] H. Aljendeel and H. Q. Hussein, "Advanced Study of Promoted Pt /SAPO-11 Catalyst for Hydroisomerization of the n-Decane Model and Lube Oil," *Iraqi Journal of Chemical and Petroleum Engineering*, vol. 22, no. 2, pp. 17–26, 2021, <https://doi.org/10.31699/IJCPE.2021.2.3>
- [17] G.K.Jabaar and H. A. Al-Jendeel, " Synthesis and characterization of SAPO-11 using carbon nanotubes", *AIP Conf. Proc.* 2806, 030016, 2023. <https://doi.org/10.1063/5.0163114>
- [18] L. Li, K. Shen, X. Huang, Y. Lin, and Y. Liu, 2021, "SAPO-11 with preferential growth along the a-direction as an improved active catalyst in long-alkane isomerization reaction," *Microporous and Mesoporous Materials*, vol. 313, <https://doi.org/10.1016/j.micromeso.2020.110827>
- [19] G. Xing, S. Liu, Q. Guan, and W. Li, 2019, "Investigation on hydroisomerization and hydrocracking of C 15 –C 18 n-alkanes utilizing a hollow tubular Ni-Mo/SAPO-11 catalyst with high selectivity of jet fuel," *Catal Today*, pp. 109–116, <https://doi.org/10.1016/j.cattod.2018.04.028>
- [20] Hammadi, A. N., and K. Shakir, I. 2019, " Adsorption Behavior of Light Naphtha Components on Zeolite (5A) and Activated Carbon". *Iraqi Journal of Chemical and Petroleum Engineering*, 20(4), 27–33, <https://doi.org/10.31699/IJCPE.2019.4.5>
- [21] V. Chandra Srivastava, 2012, "An evaluation of desulfurization technologies for sulfur removal from liquid fuels," *RSC Advances*, vol. 2, no. 3. pp. 759–783, <https://doi.org/10.1039/C1RA00309G>
- [22] Alireza Haghghat Mamaghani, Shohreh Fatemi, Mehrdad Asgari, 2013, "Investigation of Influential Parameters in Deep Oxidative Desulfurization of Dibenzothiophene with Hydrogen Peroxide and Formic Acid", *International Journal of Chemical Engineering*, vol. 2013. <https://doi.org/10.1155/2013/951045>

- [23] R. A. Omar, N. Verma, and P. K. Arora, "Sequential desulfurization of thiol compounds containing liquid fuels: Adsorption over Ni-doped carbon beads followed by biodegradation using environmentally isolated *Bacillus zhangzhouensis*," *Fuel*, vol. 277, 2020, <https://doi.org/10.1016/j.fuel.2020.118208>
- [24] Beshkoofeh S., Ghalami-Chooabar B., and Shahidian Z., 2021 "Optimization of the Oxidative Desulfurization Process of Light Cycle Oil with NiMo/ γ Al₂O₃ Catalyst", *Phys. Chem. Res.*, Vol. 10, No. 1, 57-67, 2022 <https://doi.org/10.22036/PCR.2021.285150.1917>
- [25] Li'e Jin, Qing Cao, Jinpin Li, Jinxiang Dong, 2011, "Sulfur removal in coal tar pitch by oxidation with hydrogen peroxide catalyzed by trichloroacetic acid and ultrasonic waves", *Fuel*, 90(11), 3456-3460, <https://doi.org/10.1016/j.fuel.2011.06.047>
- [26] Ahmedzek N.S., Alhassani M. H., AlMayah A.M., and Rashid H.A., "The Use of Locally Prepared Zeolite (Y) For the Removal of Hydrogen Sulfide from Iraqi Natural Gas", *Research Journal of Pharmaceutical, Biological and Chemical Sciences*, 7(6), 2016.
- [27] Ahmedzeki, N. S., and Ibrahim, B. J. Reduction of Sulfur Compounds from Petroleum Fraction Using Oxidation-Adsorption Technique. *Iraqi Journal of Chemical and Petroleum Engineering*, 16(1), 35–48, 2015. <https://doi.org/10.31699/IJCPE.2015.1.4>
- [28] A. Mojaverian Kermani, V. Mahmoodi, M. Ghahramaninezhad, and A. Ahmadpour, 2021, "Highly efficient and green catalyst of {Mo132} nanoballs supported on ionic liquid-functionalized magnetic silica nanoparticles for oxidative desulfurization of dibenzothiophene," *Sep Purif Technol*, vol. 258, <https://doi.org/10.1016/j.seppur.2020.117960>
- [29] Sama M. Al-Jubouri, Haider A. Al-Jendeel, Sarmad A. Rashid, Sirhan Al-Batty, 2023, "Green synthesis of porous carbon cross-linked Y , nanocrystals material and its performance for adsorptive removal of a methyl violet dye from water", *Microporous and Mesoporous Materials*, Volume 356, <https://doi.org/10.1016/j.micromeso.2023.112587>
- [30] B. H. Hameed, J. M. Salman, and A. L. Ahmad, 2009, "Adsorption isotherm and kinetic modeling of 2,4-D pesticide on activated carbon derived from date stones," *J Hazard Mater*, vol. 163, no. 1, pp. 121–126, <https://doi.org/10.1016/j.jhazmat.2008.06.069>
- [31] H. A. Aljandeel and H. Q. Hussein, 2018, "Kinetic Study of Hydroisomerization of n-Decane using Pt/SAPO-11 catalysts," *Iraqi Journal of Chemical and Petroleum Engineering*, vol. 19, no. 3, pp. 11–17, <https://doi.org/10.31699/ijcpe.2018.3.2>
- [32] Aljandeel, H. A., Rasheed, H. A., Ahmedzeki, N. S., Alhassani, M. H. 2023, "Dual Application of Al-Kheriat of Removal of Arsenic from Aqueous Solution and Acting as Rodenticide". *Journal of Ecological Engineering*, 24 (4), 16-26. <https://doi.org/10.12911/22998993/159335>

إزالة الكبريت من الزيت المحاكي باستخدام SAPO-11 مع الأنابيب النانوية الكربونية كمادة ماصة: دراسة حركية

غيث كريم جبار^{١*}، حيدر عبد الكريم الجندي^١، و ياسر علي الشيخ^٢

^١ قسم الهندسة الكيماوية، كلية الهندسة، جامعة بغداد، بغداد، العراق

^٢ قسم الهندسة الكيماوية والبتروكيماوية، كلية الهندسة، جامعة نزوى، سلطنة عمان

الخلاصة

تم إجراء هذا العمل لدراسة عملية إزالة الكبريت المؤكسدة لإزالة الكبريت من الزيت المقلد. تم إنتاج السيليكا والومينو فوسفات (SAPO-11) باستخدام الطريقة الحرارية المائية بتركيز من الأنابيب النانوية الكربونية (CNT) بنسبة ٠٪ و ٧,٥٪ ودرجة حرارة تبلور ١٩٠°م. تم وصف SAPO-11 المركب باستخدام حيود الأشعة السينية (XRD) و Brunauer-Emmet-Teller ؛ تم اكتشاف أن إضافة CNT زادت من تبلور SAPO-11. أظهرت النتائج أن مساحة السطحية كانت ١٧٩,٥٤ م^٢ / جم ، وكان حجم المسام ٠,٣١٧ سم^٣ / جم لنسبة CNT 7.5% ، وكانت مساحة السطحية كانت ١٢٥,٣١١ م^٢ / جم ، وكان حجم المسام ٠,٢٧٥ سم^٣ / جم بينما تم الحصول على جسيمات نانوية بمتوسط قطر جسيمي ٢٤,٨ نانومتر. في المقابل ، كان التركيب المولي النهائي لـ SAPO-11 المحضر هو Al₂O₃: 0.93P2O5: 0.414SiO₂. تم تحضير SAPO-11 / MO باستخدام طرق التثريب. بعد ذلك ، تم استخدام SAPO-11 المحضر في عملية إزالة الكبريت المؤكسدة. في هذا العمل ، تمت دراسة نزع الكبريت المؤكسد باستخدام عدة عوامل تؤثر على كفاءة إزالة الكبريت ، مثل الوقت (١٠٠، ١٢٠، ١٤٠، ١٦٠، ١٨٠، ٢٠٠) دقيقة ، كمية SAPO-11 / MO ، (٠,٣، ٠,٤، ٠,٥، ٠,٦، ٠,٧). (١٠٠ مل من زيت مقلد (١٠٠ جزء في المليون من ثنائي بنزو ثيوفين) ، وكمية بيروكسيد الهيدروجين (٤) مؤكسد / ١٠٠ مل ، وتتراوح درجة الحرارة من (٤٠ ، ٥٠ ، ٦٠ ، ٧٠ ، ٨٠ °م). أظهرت النتائج أن الزيادة في SAPO-11 / MO أدت إلى زيادة في إزالة الكبريت. كانت أفضل نسبة إزالة لمحتوى الكبريت ٩٢,٧٩٪ ، تم الحصول عليها عند ٧٠°م و ٠,٦ جرام من SAPO-11 / MO عند ٧,٥٪ CNT ، والإزالة عند ٠٪ CNT كانت ٨٢,٣٤٪ ، بينما تم تحقيق التوازن بعد ١٠٠ دقيقة. أشارت النتائج إلى أن نموذج Freundlich يصف امتزاز مركبات الكبريت بشكل أفضل من Langmuir، حيث Freundlich's R² هو ٠,٩٩٧٩ ، بينما Langmuir's R² هو ٠,٩٥٥٤.

الكلمات الدالة: نزع الكبريت، متساوي الحرارة، مساحة السطح توزيع حجم المسام، سابو -١١.